Correlated terrestrial and marine evidence for global climate changes before mass extinction at the Cretaceous–Paleogene boundary

Peter Wilf*[†‡§], Kirk R. Johnson[‡¶], and Brian T. Huber[‡‖]

*Department of Geosciences, Pennsylvania State University, University Park, PA 16802; [†]Museum of Paleontology and Department of Geological Sciences, University of Michigan, Ann Arbor, MI 48109; [¶]Department of Earth Sciences, Denver Museum of Nature & Science, Denver, CO 80205; and [‖]Department of Paleobiology, National Museum of Natural History, Smithsonian Institution, Washington, DC 20560

Edited by W. A. Berggren, Woods Hole Oceanographic Institution, Woods Hole, MA, and approved November 26, 2002 (received for review August 5, 2002)

Terrestrial climates near the time of the end-Cretaceous mass extinction are poorly known, limiting understanding of environmentally driven changes in biodiversity that occurred before bolide impact. We estimate paleotemperatures for the last ≈1.1 million years of the Cretaceous (≈66.6–65.5 million years ago, Ma) by using fossil plants from North Dakota and employ paleomagnetic stratigraphy to correlate the results to foraminiferal paleoclimatic data from four middle- and high-latitude sites. Both plants and foraminifera indicate warming near 66.0 Ma, a warming peak from ≈65.8 to 65.6 Ma, and cooling near 65.6 Ma, suggesting that these were global climate shifts. The warming peak coincides with the immigration of a thermophilic flora, maximum plant diversity, and the poleward range expansion of thermophilic foraminifera. Plant data indicate the continuation of relatively cool temperatures across the Cretaceous–Paleogene boundary; there is no indication of a major warming immediately after the boundary as previously reported. Our temperature proxies correspond well with recent pCO_2 data from paleosol carbonate, suggesting a coupling of pCO_2 and temperature. To the extent that biodiversity is correlated with temperature, estimates of the severity of end-Cretaceous extinctions that are based on occurrence data from the warming peak are probably inflated, as we illustrate for North Dakota plants. However, our analysis of climate and facies considerations shows that the effects of bolide impact should be regarded as the most significant contributor to these plant extinctions.

In contrast to the well resolved marine record (1–6), terrestrial climates near the Cretaceous–Paleogene boundary (K–P), a time marked by bolide impact (7, 8) and mass extinctions (9–15), remain poorly known. Paleobotanical reports have suggested long-term cooling across the K–P in Asia (16), no temperature change (10) or a major temperature increase soon after the boundary (17) in the Raton Basin of New Mexico and Colorado, and latest Cretaceous warming followed by a cooler Paleocene in North Dakota (18). Fine-scale correlations between continental and marine temperature records near the K–P have previously not been attempted (5, 19), though such data would help to assess the global extent of warming and cooling events as well as the correlation of partial pressure of CO_2 (pCO_2) and temperature (20, 21). Detection of climatic shifts just before the K–P would refine understanding of the mass extinction event by making it possible to distinguish the effects of climate change from those of bolide impact on biodiversity.

The most intensively sampled sequence of plant macrofossils that spans the K–P is exposed in southwestern North Dakota (19, 22). Previous estimates of K–P plant extinction in these strata range from 70 to 90% (11, 19, 23). Here, we apply recent improvements in the stratigraphic resolution, sample size, and known diversity of the North Dakota floras to produce high-resolution paleoclimatic analyses. The development of a paleomagnetic stratigraphy for the study area (22) allows us to correlate paleobotanical and marine data by using a revised time scale with a K–P age of 65.51 million years ago (Ma) (22) and 0.333-million year (m.y.) and 0.270-m.y. durations for the Cretaceous and Paleocene portions, respectively, of magnetic polarity subchron 29r (24). We present a revision of the marine record for the last ≈1.1 m.y. of the Cretaceous (Fig. 1). Floral data are then used to construct a proxy curve of mean annual temperatures for the same portion of the Cretaceous as well as the first ≈0.6 m.y. of the Paleocene (Fig. 2). We compare the terrestrial and marine results (Fig. 1*c*) and use the new climate record to reexamine the severity of plant extinctions in North Dakota.

Study Areas, Specimens, and Methods

Foraminifera. Maastrichtian paleotemperature estimates from one high-latitude and three mid-latitude deep-sea sites with reliable oxygen isotope and magnetic polarity data were correlated to a unified age model by using linear extrapolation of sedimentation rates from the K–P and paleomagnetic reversals (Fig. 1). The sites and data sources were as follows: the Bass River borehole in the New Jersey coastal plain, 40°N paleolatitude, 100 m paleodepth, data from ref. 5; Deep Sea Drilling Project Site 525A, South Atlantic, 35°S, 1,000 m, data from ref. 3; Ocean Drilling Program (ODP) Site 1050, western North Atlantic, 30°N, 1,500 m, new data; and ODP Site 690, Weddell Sea, 65°S, 1,500 m, data from ref. 4 and this study. Age models and the new data for Sites 690 and 1050 are given in Tables 1–7, which are published as supporting information on the PNAS web site, www.pnas.org. Earliest Paleocene foraminifera from these sites were not included because of problems related to stratigraphic mixing and diagenetic alteration of $\delta^{18}O$ values (28). Uncertainties of the ages and isotopic temperatures are about ±0.1 m.y. and ±2–3°C, respectively.

Fossil Plants. Our floral data are derived from more than 22,200 identified specimens of leaves and reproductive organs, collected from 161 quarries at 128 distinct stratigraphic horizons in a 183 m composite section that is calibrated to the K–P (19, 22). The section is exposed in the vicinity of Marmarth, North Dakota, in the Williston Basin at ≈49°N paleolatitude (29). The included rock units are the Cretaceous Hell Creek and the predominantly Paleocene Fort Union formations. Both represent floodplain environments; channel deposits dominate the Hell Creek locally, whereas pond and mire remains make up the bulk of the Fort Union Formation.

The K–P is recognized in the area by an iridium anomaly, shocked minerals, and a spherule layer, all thought to be products of the Chicxulub impact (11, 19, 30). These features are

EVOLUTION

This paper was submitted directly (Track II) to the PNAS office.

Abbreviations: K–P, Cretaceous–Paleogene boundary; Ma, million years ago; m.y., million year(s); pCO_2, partial pressure of carbon dioxide.

[‡]P.W., K.R.J., and B.T.H. contributed equally to this work.

[§]To whom correspondence should be addressed. E-mail: pwilf@geosc.psu.edu.

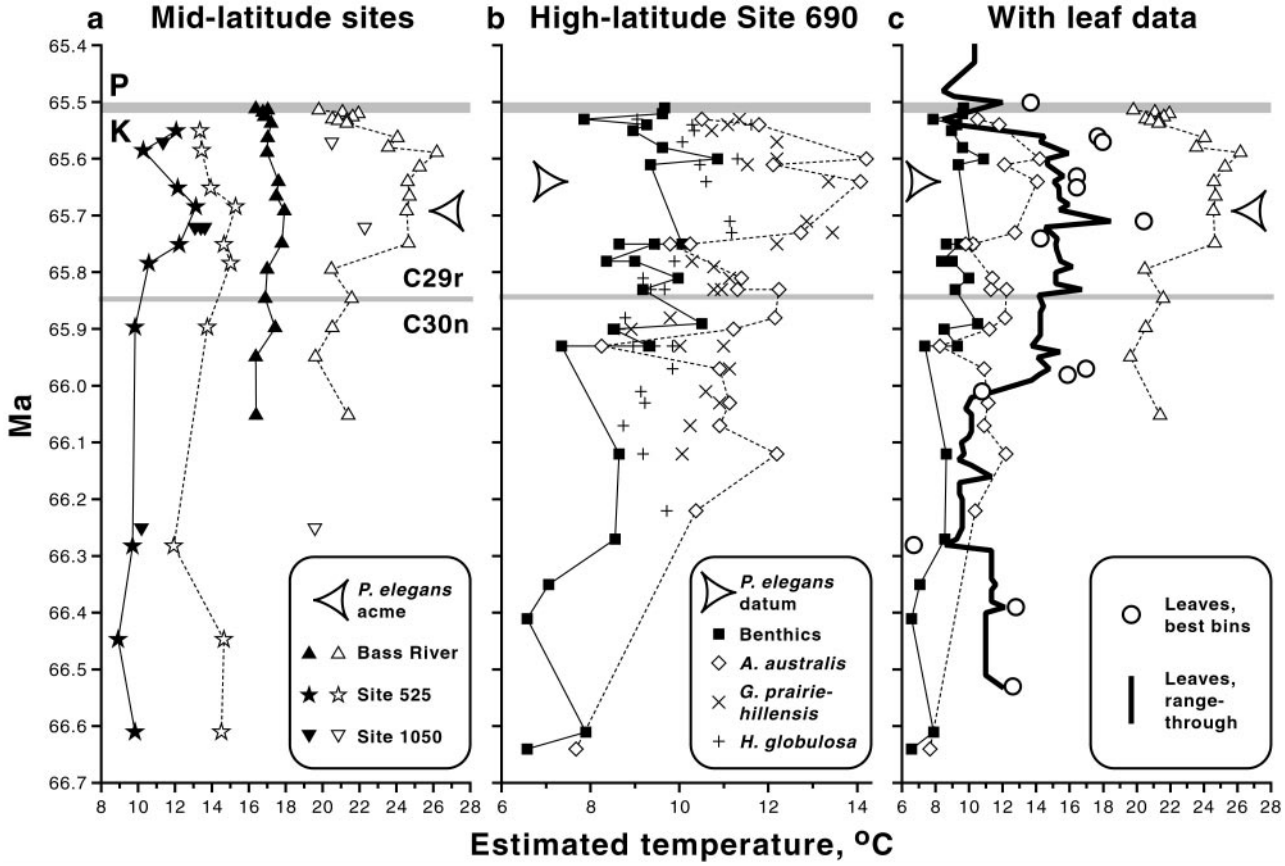

Fig. 1. Terminal Cretaceous paleotemperatures estimated from oxygen isotope data from tests of benthic (filled symbols) and planktic (open symbols) foraminifera at middle- (*a*) and high- (*b*) latitude drilling sites (see text for references), with the most complete data from *a* and *b* plotted against temperatures derived from North Dakota leaves (Fig. 2 and Table 8) (*c*). Large arrowheads indicate the Bass River size and abundance acme (5), in *a*, and the Antarctic appearance datum (2), in *b*, for *P. elegans* (see text). Paleotemperatures were calculated by using the equation of Erez and Luz (25), assuming an ice-free world with an average $\delta^{18}O$ value for ocean water of −1.2 ‰, Peedee belemnite standard (26). Benthic data are based on combined $\delta^{18}O$ values for *Gavelinella beccariiformis* and *Nuttallides truempyi*, which generally plot within 0.2 ‰ of each other. None of the data has been corrected for variations in seawater salinity or vital effects, and normal marine salinity is assumed for all sites. K = Cretaceous; P = Paleogene; C30n, C29r, C29n = magnetic polarity subchrons 30 normal, 29 reversed, and 29 normal, respectively. Limitations on graphic presentation cause floral data from 20 cm above and foraminiferal data from just below the K–P to appear within the gray line representing the K–P.

associated locally with extinctions of vertebrates, including dinosaurs (13, 31), as well as insects (15), palynomorphs (11, 30, 31), and plant macrofossil species (11, 19, 23). Macrofossils of typical Cretaceous plants occur as high as 2 m below (≪0.1 m.y. before) the K–P, and their last appearances at this level are associated with a shift to mire deposition in the Cretaceous portion of the Fort Union Formation (30, 31). Diagnostically Cretaceous palynofloras occur in the mire deposits at reduced abundance and diversity and disappear at the K–P impact horizon (30, 31). Despite differences of taxonomic resolution and taphonomy, palynomorphs and macrofossils are derived from the same source vegetation. Therefore, the loss of macrofossil species 2 m below the K–P has been interpreted primarily as a pseudoextinction related to facies change that masks a true extinction at the K–P (30, 31). Of Cretaceous macrofossil species, 70–90%, including all dominant taxa, do not reappear in any facies above the K–P (19, 23).

Our paleobotanical data are updated and revised from Johnson (19) to incorporate 13,914 additional census specimens and other new collections, resulting in an approximate doubling of the numbers of specimens and quarries used in the last paleoclimatic analysis from the Marmarth area (18), which was based on floral zones instead of an explicit age model as used here. The 386 types of plant organs recovered represent an estimated 353 species, a 43% increase. This estimate is equal to the total number of described species and undescribed morphospecies (hereafter referred to as "species" for convenience) that are represented by leaves, discriminated on the basis of details of foliar architecture (19, 32). Leaf types with discrete morphologies that have been found in organic attachment are combined in analysis here as single species. Examples are attached lateral and terminal leaflets of *Erlingdorfia montana* and *Platanites marginata*, both in the Platanaceae (33). Documentation of the flora is provided by Johnson (19), including illustrations, identification techniques, voucher specimen numbers for each species, collecting localities, and species lists for each locality. Revised species lists that correspond to this paper are archived in the Paleobiology Database, www.paleodb.org (34). All specimens were collected by K.R.J., and vouchers are housed at the Yale Peabody Museum and the Denver Museum of Nature & Science.

Our age model for paleobotanical data is that of Hicks *et al.* (22), constructed by using linear extrapolation of sedimentation rates from the K–P down to the base or up to the top of subchron 29r, respectively, for Cretaceous or Paleocene ages (Fig. 2). Neither the bottom of subchron 30n nor the top of subchron 29n is present in the section, so the modeled ages should be considered most accurate within subchron 29r, where they are each

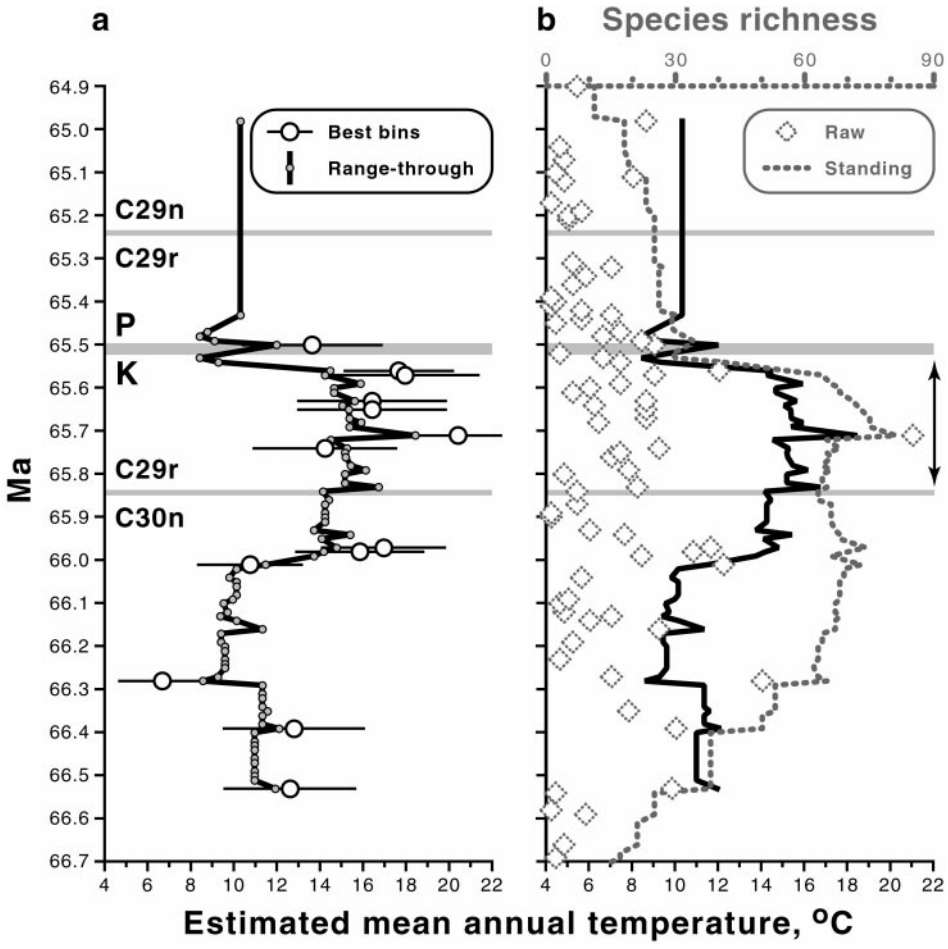

Fig. 2. Estimated paleotemperatures and floral richness for the terminal Cretaceous and earliest Paleocene in North Dakota (Table 8). (*a*) Mean annual temperatures based on leaf-margin analyses. Plots show temperatures from 13 1-m bins with at least 20 dicot leaf species each by raw count (maximum = 73 species) and 80 bins with at least 20 dicot leaf species each on a range-through basis (maximum = 92), including single-bin species (see text for details). Error bars denote $\pm 1\sigma$ of sampling error or ± 2°C, whichever is greater (27). For range-through temperatures, ± 2°C is a minimum uncertainty. (*b*) Species richness per bin as a raw count and on a standing basis exclusive of single-bin species (see text for details), plotted against range-through temperature as in *a*. Decreases in standing richness below ≈66.2 and above ≈65.2 Ma are partly artifactual as a result of edge effects (see text). Correlation of standing richness and range-through temperature from ≈66.2 to 65.5 Ma: $r = 0.605$, $P = 10^{-6}$, computed after detrending both variables by replacing each value with the difference between it and the previous value. Autocorrelations: range-through temperature, $r = 0.813$; standing richness, $r = 0.877$. Correlations with time: range-through temperature, $r = 0.341$, $P < 10^{-2}$; standing richness, $r = 0.488$, $P = 10^{-4}$. Correlation without detrending: $r = 0.511$, $P < 10^{-4}$. Arrows denote the range of the "HCIII" flora (18, 19). Abbreviations as in Fig. 1. Limitations on graphic presentation cause floral data from 20 cm above the K–P to appear within the gray line representing the K–P.

bounded by two datum points. Standard deviations on the meter levels of the base and top of subchron 29r in various section legs (22) translate via our age model to 0.107 and 0.033 m.y. for the Cretaceous and Paleocene, respectively, which can be regarded as minimum errors of our age estimates. To streamline analysis, the paleobotanical data were organized into bins of 1 m each; bin midpoints were used to derive age estimates.

Paleotemperatures were estimated by using leaf-margin analysis, a method that employs the significant correlation observed in living mesic forests between mean annual temperature and the proportion of woody dicot species with untoothed leaf margins (27, 35, 36). For fossil floras, the regression is inverted so that the proportion of untoothed species is scored as the independent and temperature computed as the dependent variable. Here we use the calibration based on East Asian forests (35, 36), which has produced estimates that are generally accurate within ± 2°C when tested on modern floras from the Americas (27, 37–39) and paleotemperature estimates for early Cenozoic floras that agree closely with other proxies (40–43). The calibration does not appear to be sensitive to pCO_2 (44), though more work is needed in this area. Promising methods have been proposed that use as many as 30 morphological characters for each species in addition to margin type (17, 45). However, in practice, the additional characters tend to add more noise than signal (27), and leaf-margin analysis generally has produced equally or more accurate temperature estimates than multivariate alternatives when tested on living forests from known climates (27, 37, 39).

Of 309 species of dicot leaves, 302, collectively represented by more than 18,000 specimens, were suitable for leaf-margin analysis because their margin states could be determined and they were probably derived from woody plants. Their occurrence data were used to derive two series of temperature estimates (Fig. 2*a*); in both cases a minimum of 20 species was used for each estimate because of the well-documented importance of sample richness for precision (27, 38). The first series was a set of conventional "spot" estimates for the 13 stratigraphic bins with 20 or more species each (maximum of 73 species). Second was a complementary series of lower-precision estimates for 80 bins with 20 or more species each on a range-through basis (maximum of 92), such that a species was considered to be present if it either (*i*) occurred in the bin or (*ii*) occurred at any pair of levels both above and below but not in the bin. The range-through approach

provides temperature estimates for intervals with no spot data and allows a more complete comparison through time of relative changes in temperature and species richness (Fig. 2*b*). The analysis assumes that a range gap is due only to sampling and not to emigration of a species followed by its immigration; this assumption undoubtedly is not valid for all gaps. However, the two data series show similar relative trends (Fig. 2*a*), suggesting that the range-through curve provides a reasonably precise complementary signal to spot data.

The spot estimates tended to be warmer than range-through data (Fig. 2*a*), probably reflecting biases favoring toothed species in the many small samples that contribute to the range-through data. The overrepresentation of toothed species in small samples could result from their high relative abundance in original vegetation (27, 38) or a toothed bias in original vegetation growing near bodies of water (38). The bins used for spot estimates comprise the best point samples of dicot richness and contain the greatest numbers of species that are found only in single bins. Within bins, these species tend to have a lower percentage of toothed margins than the bin as a whole.

In addition to leaf-margin data, we noted the presence and abundance of palms, a conventional proxy for warm winters without hard frost (46), and we plotted the range of the thermophilic "HCIII" flora (18, 19), which contains immigrant taxa from the Southern Rockies (Fig. 2*b*).

Species richness, including non-dicots (353 total species based on leaves), is plotted for comparison to temperature (Fig. 2*b*), both as (*i*) the raw number of species per bin, including the species only found in single bins, and (*ii*) the total number of range-through species exclusive of species only found in single bins, hereafter designated as "standing richness." This metric of standing richness is used because the derivation closely matches that of the range-through temperature curve used for comparison (Fig. 2*b*). Single-bin species are eliminated because they possess a number of detrimental properties for estimating standing richness (47), though they are needed in the temperature estimates to increase precision and to offset possible biases favoring the collection of toothed species. The decreases in standing richness toward the bottom and top of Fig. 2*b* are edge effects: the number of overlapping ranges diminishes artifactually near the bounds of the sampled interval. A conservative interpretation of per-capita origination and extinction rates for each bin, after Foote (47), shows that edge effects have a negligible effect on standing richness between ≈66.2 and ≈65.2 Ma (P.W. and K.R.J., unpublished data). Because they do not include range data, the raw richness data are immune to edge effects by definition.

Sampling was most intensive within ≈20 m of the K–P (19), which biases against the observation of floral richness before ≈65.9 Ma (Fig. 2*b*). The specimen count for the lowest 10 m of Paleocene strata is ≈60% greater than for the highest 10 m of the Cretaceous, which biases against the observation of a decline in richness across the K–P. The modeled ages and leaf-margin and richness data for each bin are given in Table 8, which is published as supporting information on the PNAS web site.

Results

Foraminifera. Most of the marine data indicate warming near 66.0 Ma, peak temperatures near 65.7 Ma, and cooling to prewarming temperatures less than 0.1 m.y. before the K–P (Fig. 1). At Bass River, planktic foraminifera suggest a warming of 4–5°C at ≈65.8 Ma and sustained high temperatures until just before the K–P. Within the warm interval, a thermophilic planktic foraminifer, *Pseudotextularia elegans*, expanded its range poleward and reached its maximum size and peak abundance in the western North Atlantic (Fig. 1*a*) (5). The benthic warming at Bass River is dampened by comparison to the planktic record. A surface cooling of 4–5°C, reversing the preceding warming, occurred less than 0.1 m.y. before the K–P. Planktic data (not shown) tentatively suggest the continuation of cool surface temperatures into the earliest Paleocene (5). At Site 525A, benthic and planktic records suggest a 2–3°C warming from ≈65.9 to 65.7 Ma and cooling less than 0.1 m.y. before the K–P. The coarsely spaced data from Site 1050 corroborate a warming by 65.7 Ma and cooler temperatures less than 0.1 m.y. before the K–P. In a nearby core, mass extinctions of foraminifera coincide precisely with K–P ejecta deposits (12).

Because of high latitude and finely resolved sampling, Site 690 may provide the most informative history of latest Cretaceous marine temperatures (Fig. 1*b*). A long-term cooling trend occurred over the last 50 m.y. of the Cretaceous, and the coolest deep and surface water temperatures of this interval are recorded in Site 690 sediments from ≈66.6 Ma (Fig. 1*b*) (48). Bottom and surface waters warmed near 66.2 Ma and again at ≈66.0 Ma. Peak surface and bottom water temperatures occurred between ≈65.7 and 65.6 Ma, which includes the only time when *P. elegans* is found at Site 690 (Fig. 1*b*) (2). This delayed appearance at high latitudes has also been observed at other sites in the Southern Ocean (2) and in Sweden (49), and it corresponds with a mid-latitude poleward migration of the planktonic foraminifer *Contusotruncana contusa* (50). A subsequent cooling occurred less than 0.1 m.y. before the K–P.

Fossil Plants. Temperature trends from the leaf data are mostly in close agreement with the marine record, especially within or just below subchron 29r, where the correlations are most precise (Figs. 1*c* and 2*a*); we refer below to spot estimates unless indicated. The oldest floras with 20 or more dicot species occur from ≈66.5 to 66.4 Ma and produce temperatures of 12–13°C (Fig. 2*a*). A cooler interval is indicated from ≈66.3 to 66.0 Ma, including the lowest estimate for the section, ≈7°C. This cooling is not matched by the marine data and may be partly artifactual because of an unusual mode of floral preservation: floras from this interval mostly occur in inclined point-bar deposits and are characterized by small-leaved, possibly shrubby or herbaceous plant species that generally have toothed leaves (51). Alternatively, the modeled age of this cooling may be imprecise because it is well below the base of subchron 29r, and it may instead correspond to the minimum marine temperatures from ≈66.6 Ma. In either case, a sustained and pronounced warming that strongly agrees with the marine record follows.

Temperatures increase to 16–17°C at ≈66.0 Ma. The peak of warming occurs between ≈65.8 and 65.6 Ma, accompanied by the immigration of the rich, thermophilic "HCIII" flora (18, 19) (Fig. 2*b*, arrows). Within this terminal Cretaceous warm interval, palms exceeded 5% of total specimens at four census sites of greater than 300 specimens each. The timing of the warm interval coincides with that seen in the marine record and also is synchronous with the *P. elegans* data from Bass River and Site 690 (Fig. 1*c*). The warmest estimate of the floral sequence, ≈20°C, occurs at ≈65.7 Ma and coincides with maximum plant richness (Fig. 2*b*). Temperatures near 18°C are indicated less than 0.1 m.y. before the K–P.

Range-through data suggest an abrupt subsequent cooling immediately before the K–P, coeval with marine cooling (Fig. 1*c*). Interpretation is complicated by the lack of a spot estimate due to low site richness, and the indicated ≈9°C temperatures are probably too cold. A combination of all 24 species found within the uppermost 3 m generates a more robust estimate of ≈11°C, which suggests a latest Cretaceous cooling of ≈7°C to temperatures similar to before ≈66.0 Ma. The cooling locally coincides with the deposition of mire facies of the basal Fort Union Formation (31). A ≈14°C estimate is derived from a flora 20 cm above the K–P (Fig. 2*a*), implying a slight warming immediately before or after the K–P; palms are present in this earliest Paleocene sample. Higher in our section, only range-

through estimates are possible, which give temperatures in the 9–10°C range that are similar to the minimum Cretaceous values; palms are present and comprise 7.8% of census specimens at 18 m above (≈0.2 m.y. after) the K–P. Significantly warmer climates are known from the Western Interior United States at ≈1.4 m.y. after the K–P, when tropical rainforests existed in Colorado (52).

Discussion

The congruence of the terrestrial and marine proxy data is especially strong with regard to warming beginning near 65.9–66.0 Ma, a peak of warming from ≈65.8 to 65.6 Ma, and cooling immediately before the K–P, and we interpret these as climate shifts of global extent. The correlated results from independent proxies also support the validity of the paleoclimatic methodologies used.

Our results correspond closely with recent proxy data for pCO_2 from paleosol carbonates from Canada, southern France, and elsewhere (21), which suggest a near doubling in pCO_2 at ≈0.5 m.y. before the K–P, a return to lower values immediately before the K–P, little or no change across the boundary, and another near doubling by ≈1.5 m.y. after the K–P. We note that the latter increase, if correct, is corroborated by the contemporaneous existence of Paleocene tropical rainforests in Colorado (52). These broad similarities with the most significant trends in our data suggest a close link between pCO_2 and temperature before and after the K–P. One source of CO_2 forcing was presumably Deccan volcanism on the Indian Plate (5, 53–55).

Our results do not corroborate a previously suggested warming in the Raton Basin, based on multivariate analyses, of 10°C across the K–P (17), though a smaller increase of perhaps 3°C is consistent with our data as discussed above. The floras on which the Raton Basin estimates were based have only 3–10 dicot species in each of three "Phase 3" floras and 11 and 19 species in the two "Phase 4" floras (17). These numbers are too low for reliable analysis of paleotemperature, regardless of whether univariate or multivariate methods are used (27, 38), especially for "Phase 3." Recently, Beerling *et al.* (20) provisionally suggested an increase in pCO_2 immediately after the K–P to >2,300 ppm, which presumably would have been linked to high temperatures. We regard this result, based on stomatal index values for a fern taxon (aff. *Stenochlaena*) recovered from ≤25 cm above the K–P in the Raton Basin, as speculative for the reasons stated or implied by the authors. First, the stomatal response of the fern's presumed modern relative to carbon dioxide is statistically incompatible with the results from the fossil fern, suggesting that the modern and fossil species are not closely related and may not be suitable for comparison. Second, the fossil fern has not been found in other stratigraphic horizons so as to allow calibration of its stomatal indices to baseline values. Therefore, the fossil stomatal data (20) appear to us to be reliable indicators neither of high nor low pCO_2 during the earliest Paleocene.

Climate Changes Before K–P Extinction

We examined the linkage of plant diversity in our study area with climate (Fig. 2*b*). Standing richness and range-through temperature are weakly but significantly correlated through the interval from ≈66.2 to 65.5 Ma, where correlation is possible because of negligible edge-effects on richness and nearly continuous range-through estimates of temperature; detrending was applied to mitigate the significant autocorrelations and time correlations of each variable (Fig. 2*b*). Notably, the correlation is poor before ≈66.0 Ma, when cool temperatures occur along with rich floras. The strongest correspondence is seen from ≈65.8 Ma to the K–P, when temperature and floral richness both reach maxima, diminish slightly, then decrease abruptly during the last 0.1 m.y. of the Cretaceous (Fig. 2*b*). The decrease coincides with the presence of mire deposits and the taphonomic loss of typical species of Cretaceous macrofossils (31).

Latest Cretaceous cooling probably contributed to a decline in plant richness by eliminating elements of the thermophilic flora that was present during the time of peak warmth (Fig. 2*b*, arrows). However, several lines of evidence indicate that climate change was not the principal cause of plant extinctions across the K–P. First, older Cretaceous floras were rich, despite cool climates and a relatively low intensity of sampling: five of the bins from before ≈66.0 Ma have more than 25 species each, and standing richness exceeds 60 species continuously from ≈66.3 to 65.6 Ma (Fig. 2*b*). A bin with 30 species on a raw-count basis occurs at ≈66.4 Ma and one with 50 species at ≈66.3 Ma (Fig. 2*b*), when both foraminiferal and plant data indicate cold temperatures. Paleocene floras, which grew at similar temperatures to the portion of the Cretaceous before ≈66.0 Ma, were depauperate: the richest Paleocene flora occurs in the bin immediately above the K–P, with 25 species. Second, the presence of diagnostically Cretaceous palynomorphs (30) within the mire deposits that we correlate to the terminal cool interval shows both that a major extinction related to cooling did not take place and that typical Cretaceous plants were still present but not preserved as macrofossils. This interpretation does not exclude the possibility that some species were lost because of cooling, and we note that the drop in abundance and diversity of typical Cretaceous palynomorphs within the mire deposits (30) might reflect the effects of cooling as well as facies changes. Third, the occurrence and occasional abundance of palms during the earliest Paleocene indicates that hard freezes, which could have negatively affected richness, were at most infrequent despite relatively low mean annual temperatures. This interpretation of low temperature seasonality is corroborated by the abundance of crocodilian, champsosaur, and turtle remains in correlative strata (56). Fourth, our Paleocene floras overwhelmingly bear the imprint of ecological trauma, including the loss of all Cretaceous dominant species from all facies (11, 19, 23), diminishing richness after the K–P that is in accord with continuing taxonomic losses observed in the wake of other extinction events (57), and the nearly total disappearance of specialized types of insect feeding on leaves (15). The effects of bolide impact provide the most plausible explanation for these phenomena.

In conclusion, cooling during the final 0.1 m.y. of the Cretaceous probably accounts for some loss of richness from the peak diversity of the preceding warm interval, and the relatively lower frequency of channel deposits, which were the source of the majority of the Cretaceous floras, above the K–P is also likely to inflate the apparent magnitude of extinction across the K–P. Previous observations of the loss of 70–90% of macrofossil species (23) were based, by necessity, on floras from the peak of warmth and floral diversity that are lost from the record taphonomically during the ensuing, terminal Cretaceous cooling. Conservatively, these percentages are best regarded as maximum estimates of the K–P plant extinction, whereas the 30% palynofloral extinction observed in the same strata provides a minimum estimate because of the lower taxonomic and higher stratigraphic resolution of palynofloral data (30). Our integrated terrestrial and marine climate record should help to improve understanding of the fates of other groups of organisms at the K–P boundary by expediting the discrimination of climatic from impact effects on biodiversity.

We thank K. MacLeod for providing isotopic data from Sites 690 and 1050; S. Manchester and an anonymous colleague for reviews; C. Badgley, D. Beerling, R. Burnham, R. Horwitt, C. Labandeira, B. Wilkinson, and S. Wing for detailed, helpful comments on drafts; and B. Miljour for assistance with graphics. P.W. was supported by the Petroleum Research Fund of the American Chemical Society, the Michigan Society of Fellows, and the University of Michigan Museum of Paleontology. K.R.J. received support from the Denver Museum of Nature & Science and the National Science Foundation (EAR-9805474), and B.T.H. received support from a Smithsonian Scholarly Studies Grant.

1. Stott, L. D. & Kennett, J. P. (1990) *Proc. Ocean Drill. Program Sci. Results* **113,** 829–848.
2. Huber, B. T. & Watkins, D. K. (1992) *Antarct. Res. Ser.* **56,** 31–60.
3. Li, L. Q. & Keller, G. (1998) *Geology* **26,** 995–998.
4. Barrera, E. & Savin, S. M. (1999) *Geol. Soc. Am. Spec. Pap.* **332,** 245–282.
5. Olsson, R. K., Wright, J. D. & Miller, K. G. (2001) *J. Foram. Res.* **31,** 275–282.
6. Abramovich, S. & Keller, G. (2002) *Palaeogeogr. Palaeoclimatol. Palaeoecol.* **178,** 145–164.
7. Alvarez, L. W., Alvarez, W., Asaro, F. & Michel, H. V. (1980) *Science* **208,** 1095–1108.
8. Krogh, T. E., Kamo, S. L., Sharpton, V. L., Marin, L. E. & Hildebrand, A. R. (1993) *Nature* **366,** 731–734.
9. Tschudy, R. H., Pillmore, C. L., Orth, C. J., Gilmore, J. S. & Knight, J. D. (1984) *Science* **225,** 1030–1032.
10. Wolfe, J. A. & Upchurch, G. R. (1986) *Nature* **324,** 148–152.
11. Johnson, K. R., Nichols, D. J., Attrep, M., Jr., & Orth, C. J. (1989) *Nature* **340,** 708–711.
12. Norris, R. D., Huber, B. T. & Self-Trail, J. (1999) *Geology* **27,** 419–422.
13. Sheehan, P. M., Fastovsky, D. E., Barreto, C. & Hoffmann, R. G. (2000) *Geology* **28,** 523–526.
14. Vajda, V., Raine, J. I. & Hollis, C. J. (2001) *Science* **294,** 1700–1702.
15. Labandeira, C. C., Johnson, K. R. & Wilf, P. (2002) *Proc. Natl. Acad. Sci. USA* **99,** 2061–2066.
16. Krassilov, V. A. (1975) *Palaeogeogr. Palaeoclimatol. Palaeoecol.* **17,** 157–172.
17. Wolfe, J. A. (1990) *Nature* **343,** 153–156.
18. Johnson, K. R. & Hickey, L. J. (1990) *Geol. Soc. Am. Spec. Pap.* **247,** 433–444.
19. Johnson, K. R. (2002) *Geol. Soc. Am. Spec. Pap.* **361,** 329–391.
20. Beerling, D. J., Lomax, B. H., Royer, D. L., Upchurch, G. R. & Kump, L. R. (2002) *Proc. Natl. Acad. Sci. USA* **99,** 7836–7840.
21. Nordt, L., Atchley, S. & Dworkin, S. I. (2002) *Geology* **30,** 703–706.
22. Hicks, J. F., Johnson, K. R., Obradovich, J. D., Tauxe, L. & Clark, D. (2002) *Geol. Soc. Am. Spec. Pap.* **361,** 35–55.
23. Johnson, K. R. (1992) *Cretaceous Res.* **13,** 91–117.
24. D'Hondt, S., Herbert, T. D., King, J. & Gibson, C. (1996) *Geol. Soc. Am. Spec. Pap.* **307,** 303–317.
25. Erez, J. & Luz, B. (1983) *Geochim. Cosmochim. Acta* **47,** 1025–1031.
26. Shackleton, N. J. & Kennett, J. P. (1975) *Initial Rep. Deep Sea Drill. Proj.* **29,** 743–755.
27. Wilf, P. (1997) *Paleobiology* **23,** 373–390.
28. MacLeod, K. G., Huber, B. T. & Fullagar, P. D. (2001) *Geology* **29,** 303–306.
29. Hay, W. W., De Conto, R., Wold, C. N., Wilson, K. M., Voigt, S., Schultz, M., Wold-Rossby, A., Dullo, W.-C., Ronov, A. B., Balukhovsky, A. N. & Söding, E. (1999) *Geol. Soc. Am. Spec. Pap.* **332,** 1–47.
30. Nichols, D. J. & Johnson, K. R. (2002) *Geol. Soc. Am. Spec. Pap.* **361,** 95–143.
31. Pearson, D. A., Schaefer, T., Johnson, K. R. & Nichols, D. J. (2001) *Geology* **29,** 39–42.
32. Ash, A. W., Ellis, B., Hickey, L. J., Johnson, K. R., Wilf, P. & Wing, S. L. (1999) *Manual of Leaf Architecture: Morphological Description and Categorization of Dicotyledonous and Net-Veined Monocotyledonous Angiosperms* (Smithsonian Institution, Washington, DC).
33. Johnson, K. R. (1996) *Proc. Denver Mus. Nat. Hist. Ser. 3* **3,** 1–48.
34. Alroy, J., Marshall, C. R., Bambach, R. K., Bezusko, K., Foote, M., Fürsich, F. T., Hansen, T. A., Holland, S. M., Ivany, L. C., Jablonski, D., *et al.* (2001) *Proc. Natl. Acad. Sci. USA* **98,** 6261–6266.
35. Wolfe, J. A. (1979) *U. S. Geol. Surv. Prof. Pap.* **1106,** 1–37.
36. Wing, S. L. & Greenwood, D. R. (1993) *Philos. Trans. R. Soc. London Ser. B* **341,** 243–252.
37. Wiemann, M. C., Manchester, S. R., Dilcher, D. L., Hinojosa, L. F. & Wheeler, E. A. (1998) *Am. J. Bot.* **85,** 1796–1802.
38. Burnham, R. J., Pitman, N. C. A., Johnson, K. R. & Wilf, P. (2001) *Am. J. Bot.* **88,** 1096–1102.
39. Gregory-Wodzicki, K. M. (2000) *Paleobiology* **26,** 668–688.
40. Wolfe, J. A. & Poore, R. Z. (1982) in *Climate in Earth History* (Natl. Acad. Press, Washington, DC), pp. 154–158.
41. Hutchison, J. H. (1982) *Palaeogeogr. Palaeoclimatol. Palaeoecol.* **37,** 149–164.
42. Wing, S. L., Bao, H. & Koch, P. L. (2000) in *Warm Climates in Earth History*, eds. Huber, B. T., MacLeod, K. & Wing, S. L. (Cambridge Univ. Press, Cambridge, U.K.), pp. 197–237.
43. Wilf, P. (2000) *Geol. Soc. Am. Bull.* **112,** 292–307.
44. Gregory, K. M. (1996) *Palaeogeogr. Palaeoclimatol. Palaeoecol.* **124,** 39–51.
45. Wolfe, J. A. (1995) *Annu. Rev. Earth Plan. Sci.* **23,** 119–142.
46. Greenwood, D. R. & Wing, S. L. (1995) *Geology* **23,** 1044–1048.
47. Foote, M. (2000) *Paleobiology* **26S,** 74–102.
48. Huber, B. T., Norris, R. D. & MacLeod, K. G. (2002) *Geology* **30,** 123–126.
49. Malmgren, B. A. (1982) *Geol. Foeren. Stockholm Foerh.* **103,** 357–375.
50. Kucera, M. & Malmgren, B. A. (1998) *Palaeogeogr. Palaeoclimatol. Palaeoecol.* **138,** 1–15.
51. Johnson, K. R. (1998) *Am. J. Bot.* **85** (Suppl. 6), 75.
52. Johnson, K. R. & Ellis, B. (2002) *Science* **296,** 2379–2383.
53. Caldeira, K. & Rampino, M. R. (1990) *Geophys. Res. Lett.* **17,** 1299–1302.
54. Bhandari, N., Shukla, P. N., Ghevariya, Z. G. & Sundaram, S. M. (1995) *Geophys. Res. Lett.* **22,** 433–436.
55. Courtillot, V., Gallet, Y., Rocchia, R., Féraud, G., Robin, E., Hofmann, C., Bhandari, N. & Ghevariya, Z. G. (2000) *Earth Planet. Sci. Lett.* **182,** 137–156.
56. Bryant, L. J. (1989) *Univ. Calif. Publ. Geol. Sci.* **134,** 1–107.
57. Jablonski, D. (2002) *Proc. Natl. Acad. Sci. USA* **99,** 8139–8144.